




## Article

# Design-of-Experiment-Guided Establishment of a Fermentative Bioprocess for Biomass-Bound Astaxanthin with *Corynebacterium glutamicum*

Florian Meyer <sup>1,†</sup>, Ina Schmitt <sup>1,†</sup> , Thomas Schäffer <sup>2</sup>, Volker F. Wendisch <sup>1</sup>  and Nadja A. Henke <sup>1,\*</sup> 

<sup>1</sup> Genetics of Prokaryotes, Faculty of Biology and CeBiTec, Bielefeld University, 33615 Bielefeld, Germany; volker.wendisch@uni-bielefeld.de (V.F.W.)

<sup>2</sup> Fermentation Technology, Technical Faculty and CeBiTec, Bielefeld University, 33615 Bielefeld, Germany

\* Correspondence: n.henke@uni-bielefeld.de

† These authors contributed equally to this work.

**Abstract:** *Corynebacterium glutamicum* is prominent in the industrial production of secreted amino acids. Notably, it naturally accumulates the carotenoid pigment decaprenoxanthin in its membranes. Metabolic engineering enabled the production of astaxanthin. Here, a bioprocess for astaxanthin production in lab-scale stirred bioreactors was established by a DoE-guided approach to optimize the basic process parameters pH, rDOS, aeration rate as well as inoculation cell density. The DoE-guided approach to characterize 2 L scale cultivation revealed that the pH showed the strongest effect on the product formation. Subsequently, an optimum at pH 8, an aeration rate of 0.25 vvm, 30% rDOS and an initial optical density of 1 was established that allowed production of  $7.6 \pm 0.6 \text{ mg L}^{-1}$  astaxanthin in batch mode. These process conditions were successfully transferred to a fed-batch process resulting in a high cell density cultivation with up to  $60 \text{ g CDW L}^{-1}$  biomass and  $64 \text{ mg L}^{-1}$  astaxanthin and thus demonstrating an about 9-fold improvement compared to optimal batch conditions. Moreover, pH-shift experiments indicate that the cells can quickly adapt to a change from pH 6 to 8 and start producing astaxanthin, showing the possibility of biphasic bioprocesses for astaxanthin production.

**Keywords:** design of experiment (DoE); astaxanthin; batch and fed-batch fermentation; *Corynebacterium glutamicum*



**Citation:** Meyer, F.; Schmitt, I.; Schäffer, T.; Wendisch, V.F.; Henke, N.A. Design-of-Experiment-Guided Establishment of a Fermentative Bioprocess for Biomass-Bound Astaxanthin with *Corynebacterium glutamicum*. *Fermentation* **2023**, *9*, 969. <https://doi.org/10.3390/fermentation9110969>

Academic Editors: Xidong Ren and Deqiang Zhu

Received: 13 October 2023

Revised: 4 November 2023

Accepted: 9 November 2023

Published: 11 November 2023



**Copyright:** © 2023 by the authors. Licensee MDPI, Basel, Switzerland. This article is an open access article distributed under the terms and conditions of the Creative Commons Attribution (CC BY) license (<https://creativecommons.org/licenses/by/4.0/>).

## 1. Introduction

Astaxanthin is a red C40 carotenoid with an extraordinary antioxidant activity [1]. It belongs to the xanthophyll group of carotenoids, as it contains oxygen in the form of a keto and hydroxyl group on each ionone ring. The structural properties of astaxanthin enable strong antioxidative properties in addition to high free radical scavenging and singlet oxygen-quenching activity [2]. Synthetic astaxanthin is traditionally used as a feed colorant for poultry and is the major carotenoid used in aquatic feed formulations, e.g., for salmon, rainbow trout and crustaceans [3]. In addition, natural astaxanthin is used as a colorant and antioxidant in the food and cosmetics industry, respectively. In recent years, potential medical applications of astaxanthin have attracted a lot of interest, since astaxanthin was shown to exhibit anti-inflammatory, anti-apoptotic, anti-tumor and immune-modulating properties, turning it into a potential therapeutic for, e.g., cancer [4], cardiovascular, liver and ocular diseases [5–8] as well as Alzheimer’s [9] and Parkinson’s diseases [10]. Although it is not used as a pharmaceutical yet, natural astaxanthin has become prominent as a health-promoting nutraceutical. Due to its attractive properties and commercial value, the global astaxanthin market is predicted to reach about USD 5 billion in 2028, with an annual growth rate of approximately 17% [11]. At the present time, astaxanthin sourced from petrochemical synthesis dominates the market, as it is the cheapest production method [11–13]. However, the nutraceutical, food and cosmetics industries only use naturally sourced

astaxanthin [14]. Thus, rising consumer demand has facilitated research on alternative and microbial production processes that are both environmentally friendly and scalable. High-level astaxanthin production has been enabled in a range of natural and heterologous microbial hosts like *Yarrowia lipolytica* [15,16], *Phaffia rhodozyma* [16], *Saccharomyces cerevisiae* [17], *Paracoccus carotinifaciens* [18], *Escherichia coli* [19,20], and *Corynebacterium glutamicum* [21]. Recently, an astaxanthin oleoresin extracted from *C. glutamicum* biomass was demonstrated to have an about 9-fold higher antioxidant activity than synthetic astaxanthin [22].

*C. glutamicum* naturally synthesizes the yellow C50 carotenoid decaprenoxanthin and its glucosides [23]. Over the past decade, *C. glutamicum* has been metabolically engineered for efficient production of various carotenoids [24–26] and related short-chain terpenoids [27–29]. Rational engineering to enable an improved precursor biosynthesis [26], deregulation of the native carotenoid biosynthesis [21,25,30] and abolishment of competing pathways [26] has been applied to provide high flux to the astaxanthin precursor lycopene.

For overproduction of the heterologous astaxanthin, first  $\beta$ -carotene production was established by introduction of the lycopene cyclase gene *crtY* from *Pantoea ananatis* [26]. Furthermore, conversion of  $\beta$ -carotene to astaxanthin was established and later improved by a fusion protein comprising the heterologous  $\beta$ -carotene hydroxylase and  $\beta$ -carotene ketolase from *Fulvamarina pelagi* [21] (Figure 1). Recently, a genome-mining approach with subsequent screening of structurally distinct lycopene  $\beta$ -cyclases revealed that higher astaxanthin production can be achieved with cytosolic lycopene  $\beta$ -cyclase from *Synechococcus elongatus* and membrane-bound heterodimeric lycopene  $\beta$ -cyclase from *Brevibacterium linens* [31]. Besides the targeted carotenoid pathway engineering, a systematic CRISPRi library screening identified new genetic targets from central metabolism for optimized carotenoid production. These results further hinted at the effects that seemingly unrelated pathways as well as global regulators can have on carotenoid synthesis and thus also showed the possibility of influencing these through external means, i.e., fermentation parameters or media composition [32]. Apart from the genetic engineering, several other ways of optimizing astaxanthin production were performed previously in *C. glutamicum*. As it is typically used for amino acid production, a co-production of astaxanthin and L-lysine was established and tested in a 15 L fed-batch fermentation using complex medium [33]. Additionally, we previously published both a batch and fed-batch fermentation process using a minimal medium with the optional addition of aquaculture sidestreams in a 2 L scale [34].

However, both processes suffered from low astaxanthin titers below 10 mg/L. As such, we determined that further optimization is necessary to reach commercially relevant product titers.

Industrial-scale biotechnological production processes with *C. glutamicum* have been well established in the industry for several decades, as it is used in high-titer production of several amino acids including L-lysine [35] and L-glutamate [36]. As amino acids are secreted products, the cell densities in large-scale production processes are deliberately limited [37]. By contrast, carotenoids are biomass-bound products [33]. Hence, a high cell density production process is aimed at for astaxanthin production. For *C. glutamicum*, mineral salts, high cell density cultivation (HCDC) media were developed with lignocellulosic acetate [38] or glucose [39] as carbon sources and tested for recombinant protein [40] and L-lysine production, respectively.

For bioprocess intensification, different approaches could be applied. Although laborious, one-factor-at-a-time experiments are still widely used to identify important process variables. However, this makes it impossible to identify combinatorial effects, and a large number of experiments are necessary to fully explore the experimental space. Design of experiment (DoE) approaches allow both the identification of combinatorial effects and the minimization of the number of necessary experiments and have therefore been applied, especially in bioprocess optimization, as each experiment represents a large investment of time and resources [41,42]. DoE represents a well-established methodology to plan

a series of experiments in order to elucidate the impact and correlation of a number of different test variables to a response variable. Therefore, a DoE approach is suitable to investigate the impact of different bioprocess parameters. It is well known that pH [41,43], aeration rate and rDOS [44] as well as initial inoculum [45] can have wide-ranging effects on fermentation processes and can be key to enhancing product yields.

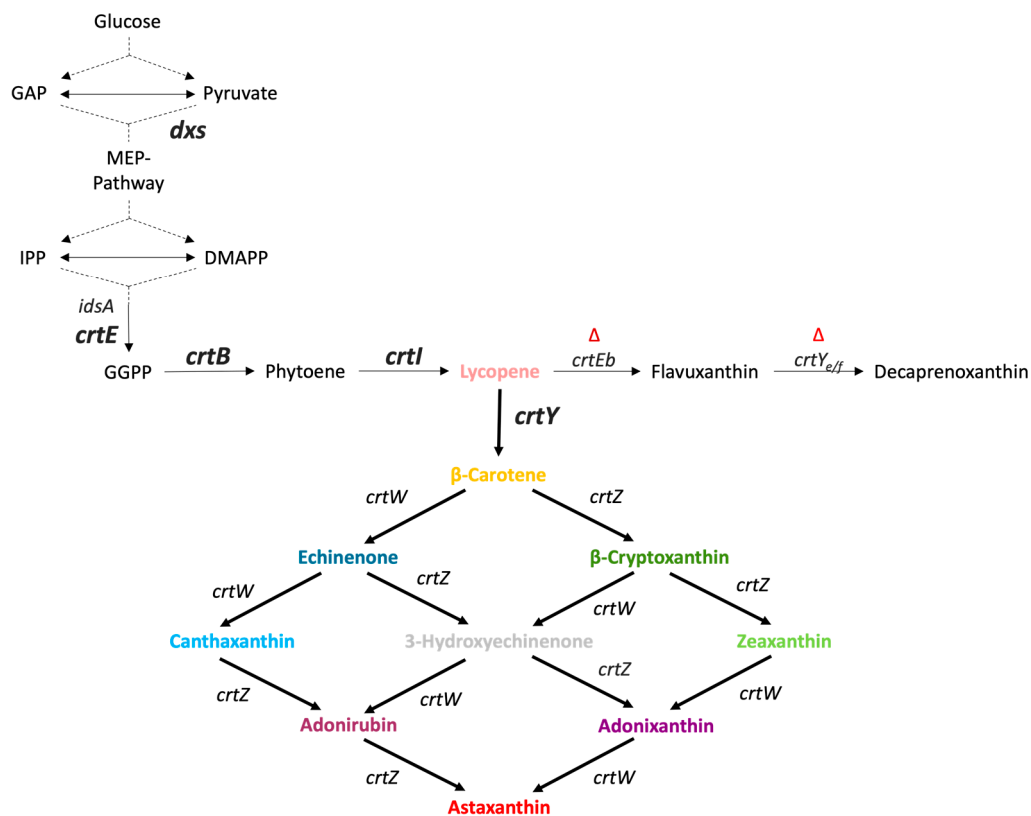


**Figure 1.** Carotenoid biosynthesis in *C. glutamicum* ASTA\*. Gene names are given next to the reactions catalyzed by their gene products; genes overexpressed from the genome are marked in bold, while deleted native genes are marked with a red  $\Delta$  above them. GAP: Glyceraldehyde 3-phosphate; IPP: isopentenyl pyrophosphate; DMAPP: dimethylallyl diphosphate; *dxs*: 1-deoxy-D-xylulose 5-phosphate synthase; *idsA*: geranylgeranyl pyrophosphate synthetase; *crtE*: geranylgeranyl pyrophosphate synthase; *crtB*: phytoene synthase; *crtI*: phytoene desaturase; *crtEb*: lycopene elongase; *crtY<sub>eff</sub>*:  $\epsilon$ -cyclase; *crtY*: lycopene  $\beta$ -cyclase from *Pantoea ananatis*; *crtW*:  $\beta$ -carotene ketolase from *Fulvimarina pelagi*; *crtZ*:  $\beta$ -carotene hydroxylase from *Fulvimarina pelagi*.

This is why, in this study, we chose these four parameters and analyzed their effects on astaxanthin production with *C. glutamicum* using a fractional factorial design in batch and fed-batch fermentations. The initial setpoints and their ranges were chosen in accordance with previously published fermentations of *C. glutamicum* (e.g., [34,44]) and varied by 50% in both directions, with the exception of pH, to allow a large-enough range to observe effects. The pH was only varied by 1 pH unit from 7 in both directions to keep it within the physiological limitations of *C. glutamicum* (e.g., [46]).

## 2. Materials and Methods

### 2.1. Preculture Conditions

All cultivations and fermentations in this study were performed with *C. glutamicum* ASTA\* [21]. Chemicals were delivered by Carl Roth (Karlsruhe, Germany) or VWR International (Radnor, PA, USA), if not stated differently. For inoculation of the bioreactor cultivations, a first pre-culture was grown in 50 mL LB medium [47] with addition of 10 g L<sup>-1</sup> glucose and 25  $\mu$ g mL<sup>-1</sup> kanamycin in a 500 mL shake flask. An appropriate

number of second pre-cultures in 200 mL CGXII minimal medium (20 g L<sup>-1</sup> (NH<sub>4</sub>)<sub>2</sub>SO<sub>4</sub>, 1 g L<sup>-1</sup> K<sub>2</sub>HPO<sub>4</sub>, 1 g L<sup>-1</sup> KH<sub>2</sub>PO<sub>4</sub>, 5 g L<sup>-1</sup> urea, 42 g L<sup>-1</sup> MOPS buffer, 0.2 mg L<sup>-1</sup> biotin, 30 mg L<sup>-1</sup> protocatechuic acid (PCA), 10 mg L<sup>-1</sup> CaCl<sub>2</sub>, 250 mg L<sup>-1</sup> MgSO<sub>4</sub>·7 H<sub>2</sub>O, trace elements: 10 mg L<sup>-1</sup> FeSO<sub>4</sub>·7 H<sub>2</sub>O, 10 mg L<sup>-1</sup> MnSO<sub>4</sub>·H<sub>2</sub>O, 0.02 mg L<sup>-1</sup> NiCl<sub>2</sub>·6 H<sub>2</sub>O, 0.313 mg L<sup>-1</sup> CuSO<sub>4</sub>·5 H<sub>2</sub>O, 1 mg L<sup>-1</sup> ZnSO<sub>4</sub>·7 H<sub>2</sub>O) [48], supplemented with 40 g L<sup>-1</sup> glucose and 25 µg mL<sup>-1</sup> kanamycin in 2 L shake flasks were inoculated with 1% (v/v) of the first preculture. The precultures were grown overnight at 30 °C and 120 rpm. Second precultures were combined for inoculation of bioreactors.

## 2.2. Fermentative Production

Glass bioreactors with a total volume of 3.7 L (KLF, Bioengineering AG, Wald, Switzerland) were used for all fermentations. The stirrer-to-reactor diameter ratio was 0.39, and the aspect ratio of the reactor was 2.6:1.0. The temperature was kept at 30 °C during the fermentations. Samples during the fermentations were collected with autosamplers and cooled down to 4 °C until further use. A Shimadzu UV-1202 spectrophotometer (Duisburg, Germany) was used for OD<sub>600nm</sub> measurements. When required, cell dry weight was calculated by dividing OD<sub>600nm</sub> by four.

### 2.2.1. Batch Conditions

For the batch fermentations, two six-bladed Rushton turbines were placed on the stirrer axis with a distance of 6 and 12 cm from the bottom of the reactor. A steady airflow of 0.15 to 0.75 NL min<sup>-1</sup> (specified for each experiment in the results section) was maintained from the bottom through a ring sparger. Automatic control of the stirrer speed between 400 and 1250 rpm kept the relative dissolved oxygen saturation (rDOS) at a given level between 15 and 45% (specified for each experiment in the results section). A pH of 6.0 to 8.5 (specified for each experiment in the results section) was automatically maintained by the addition of 10% (v/v) H<sub>3</sub>PO<sub>4</sub> and 4 M KOH. Off-gas CO<sub>2</sub> was measured using a MF420-IR-CO<sub>2</sub> sensor (LogiDataTech Systems, Baden-Baden, Germany) with a measuring range from 0 to 5% (v/v) CO<sub>2</sub>. An initial working volume of 2 L CGXII medium without MOPS buffer, supplemented with 40 g L<sup>-1</sup> glucose, 25 µg mL<sup>-1</sup> kanamycin and 0.6 mL L<sup>-1</sup> antifoam 204 (Sigma-Aldrich; St. Louis, MO, USA) was inoculated to an OD<sub>600nm</sub> of 0.5 to 2 (specified for each experiment in the results section) from the second pre-culture.

### 2.2.2. Fed-Batch Conditions

For the fed-batch fermentations, three six-bladed Rushton turbines were placed on the stirrer axis with a distance of 6, 12 cm and 18 cm from the bottom of the reactor. Furthermore, a mechanical foam breaker was installed on the stirrer axis with a distance of 22 cm to the bottom of the reactor. The fed-batch fermentations were performed with a head space overpressure of 0.5 bar. A pH of 7.0 or 8.0 was automatically maintained by the addition of 10% (v/v) H<sub>3</sub>PO<sub>4</sub> and 25% (v/v) NH<sub>3</sub>. The fed-batch fermentations were performed with an initial working volume of 1 L HCDC medium (10 g L<sup>-1</sup> glucose, 19.75 g L<sup>-1</sup> KH<sub>2</sub>PO<sub>4</sub>, 39.5 g L<sup>-1</sup> K<sub>2</sub>HPO<sub>4</sub>, 10 g L<sup>-1</sup> (NH<sub>4</sub>)<sub>2</sub>SO<sub>4</sub>, 6.67 g L<sup>-1</sup> MgSO<sub>4</sub>·7 H<sub>2</sub>O, 0.27 g L<sup>-1</sup> CaCl<sub>2</sub>, 0.53 g L<sup>-1</sup> FeSO<sub>4</sub>·7 H<sub>2</sub>O, 0.27 g L<sup>-1</sup> MnSO<sub>4</sub>·H<sub>2</sub>O, 0.027 g L<sup>-1</sup> ZnSO<sub>4</sub>·7 H<sub>2</sub>O, 0.0053 g L<sup>-1</sup> CuSO<sub>4</sub>, 0.00053 g L<sup>-1</sup> NiCl<sub>2</sub>·6 H<sub>2</sub>O, 0.0053 g L<sup>-1</sup> d(+)-biotin, 0.8 g L<sup>-1</sup> PCA) [39], inoculated to an OD<sub>600nm</sub> of 1 with the second pre-culture. One L of 600 g L<sup>-1</sup> glucose was used as feed medium. An automatic control increased the stirrer speed from 400 to 1500 rpm every time the relative dissolved oxygen saturation (rDOS) fell below 30%. The feed was primed when the rDOS fell below 30% for the first time. The feed pump activated every time the rDOS exceeded 60% and stopped when it subsequently fell below 60%, to prevent oversaturation with glucose. A steady airflow of 0.3 to 3.5 NL min<sup>-1</sup> was maintained from the bottom through a ring sparger. The airflow was increased manually during the process when the rDOS fell below the desired limit and the agitator was already at its maximum. Foam formation during the fermentation was reduced by addition of 0.6 mL L<sup>-1</sup> antifoam 204 to

the batch medium and controlled addition of up to 30 mL antifoam 204 via an antifoam probe during the feeding phase.

### 2.3. Quantification of Carotenoids, Carbohydrates and Organic Acids

For all HPLC analyses, an Agilent 1200 series system (Agilent Technologies Deutschland GmbH, Böblingen, Germany) was used. Culture samples (200 or 500 µL) were centrifuged at 14,000 rpm for 10 min, and the supernatants and pellets were stored separately at −20 °C until analysis.

The analysis of carotenoids was performed as previously described [49]. Samples were extracted until the remaining pellet of cell debris was colorless. Carotenoid analysis was performed for all fermentations carried out during this study. For quantification of the carotenoid contents, the peak areas detected at 471 nm and calibration curves calculated from authentic standards were used. Astaxanthin, adonirubin, canthaxanthin, echinenone, β-cryptoxanthin, zeaxanthin, β-carotene and lycopene were quantified by comparing the peak area against that of authentic standards. Hydroxyechinenone was calculated as astaxanthin equivalent as there was no authentic standard available. Furthermore, total carotenoids were calculated by converting all measured carotenoid titers to mmol, adding them and then converting back to mg/L of astaxanthin.

The carbohydrates in the cultivation medium were quantified with an organic acid resin column (Organic acid, 300 mm × 8 mm, 10 µm particle size, 25 Å pore diameter; CS-Chromatographie Service GmbH, Langerwehe, Germany) under isocratic conditions with a flow of 0.8 mL min<sup>−1</sup> 5 mM H<sub>2</sub>SO<sub>4</sub>. The analytes were detected using a refractive index detector (RID).

### 2.4. Design of Experiments Setup and Statistical Analysis

The fractional factorial design was generated using R and the rsm package [50,51]. To identify the influence of the factors pH, rDOS, aeration and initial inoculum, we used a fractional factorial cube design (Table 1). The effect of the initial inoculum was confounded with the combined effect of the other three factors (Table 2). Two center points were performed in addition, to test for potential higher-level effects. Either the maximum astaxanthin or total carotenoid titer during the process were chosen as response variables.

**Table 1. Overview over the tested bioprocess parameters and their respective levels.** Levels were chosen based on previously performed fermentations and physiological limitations of *C. glutamicum*.

Modified Parameter	Level		
	−1	0	+1
Aeration [vvm]	0.25	0.5	0.75
Initial OD <sub>600nm</sub> [−]	1	3	5
pH [−]	6	7	8
rDOS [%]	15	30	45

**Table 2. Overview of randomized DoE fermentation runs.** The rDOS, aeration rate and pH setpoint, as well as the initial OD<sub>600nm</sub> for each fermentation, are stated. Control runs are marked gray. n.d. = not detectable.

Run	rDOS [%]	Aeration Rate [vvm]	Initial OD <sub>600nm</sub>	pH	Astaxanthin Titer [mg L <sup>−1</sup> ]	Total Carotenoids as Astaxanthin Equivalents [mg L <sup>−1</sup> ]	Max. CDW [g L <sup>−1</sup> ]
1	30	0.50	3	7	1.79	19.57	13
2	15	0.75	5	6	0.66	103.71	5.25
3	45	0.25	1	8	8.19	16.67	9.5
4	45	0.75	5	8	7.47	26.20	9.25
5	15	0.25	5	8	9.84	21.62	10.25
6	45	0.25	5	6	0.33	19.65	7
7	30	0.50	3	7	4.45	15.24	8
8	15	0.25	1	6	0.41	189.77	12.25
9	15	0.75	1	8	6.49	14.95	8.5
10	45	0.75	1	6	n.d.	10.20	4.25



### 3. Results

#### 3.1. Design of Experiments for rDOS, Aeration Rate, Initial OD<sub>600nm</sub> and pH

To identify the influence of rDOS, aeration rate, initial OD<sub>600nm</sub> and pH on the astaxanthin production process, 10 batch fermentations were performed in CGXII medium. These were organized in a fractional cube design and initially based on our previously published batch fermentations [34]. Maximum astaxanthin titers from these runs are shown in Table 2 and Figure 2. In addition, total carotenoid titers were determined and given as astaxanthin equivalents, as described in the methods section. These results showed that pH 6 almost completely abolished the formation of any xanthophylls, while pH 8 is beneficial for astaxanthin formation. Effects from the other parameters are harder to distinguish.

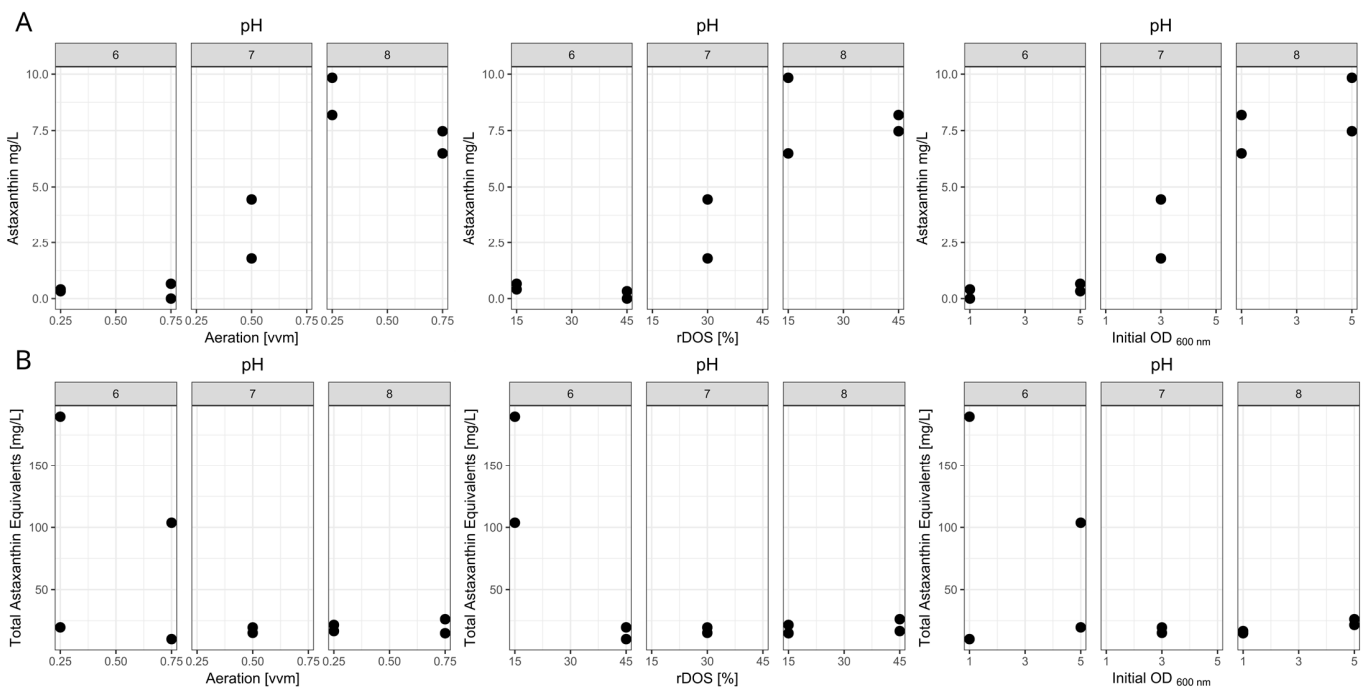


**Figure 2.** Dotplots of the DoE results clustered by pH value. These graphs represent the results of the DoE fermentations for maximal astaxanthin titers (A) and total carotenoid titers given as astaxanthin equivalents (B). Results are clustered by pH value to enhance readability. Fermentations were performed in a 2 L CGXII medium using *C. glutamicum* ASTA\* at 30 °C. pH was controlled using 4 M KOH and 10% H<sub>3</sub>PO<sub>4</sub>. Aeration, rDOS, pH and initial OD<sub>600nm</sub> were varied according to the design-of-experiment approach.

To facilitate the analysis of the data, we tried fitting a first- or second-order model. When fitting the latter model, the effect of the two-factor interactions was not significant (Prob > F of 0.82). The first order model, however, showed a significant fit (Prob > F of 0.003) and a non-significant lack of fit (Prob > F of 0.86). Additionally, it had an adjusted R<sup>2</sup> of 0.89, meaning the first-order model can explain 89% of the measured variability. Relevant statistical outputs of the regression analysis are shown in Table 3. Overall, the set of DoE fermentations showed a high variance with astaxanthin titers ranging from 0 to 9.84 mg L<sup>-1</sup> astaxanthin. The ANOVA indicated a highly significant effect of the pH with regard to the astaxanthin titer, while the other tested variables, namely aeration rate, rDOS and initial OD<sub>600nm</sub>, showed no significant effects. To further analyze if the pH was masking other potentially significant effects, we also performed a Student's *t*-test to only compare changes at the same pH level (Table 4). However, even under these conditions the parameters were not found to be significant.

**Table 3. Overview of the regression model and its components.** Models for both astaxanthin titer and total carotenoid titer (given as astaxanthin equivalents) are shown. The shown two-factor interactions are confounded due to the model design and cannot therefore be analyzed separately. These are shown by stars (\*) to indicate the interaction and / to indicate the aliasing between the two pairs. Furthermore, the two-factor interaction was not included for the astaxanthin model, as it only increased the lack of fit. Statistical significances were calculated using either the Student’s *t*-test (*t*-values and corresponding probabilities) or Fisher’s test (*F*-value and corresponding probabilities).

Total Carotenoids		Astaxanthin		Source
Prob > <i>t</i>	<i>t</i> -value	Prob > <i>t</i>	<i>t</i> -value	
0.36	−1.03	0.29	−1.17	Aeration
0.54	−0.67	0.41	0.91	Initial OD <sub>600nm</sub>
0.05	−2.72	<0.001	8.64	pH
0.05	−2.87	0.71	−0.4	rDOS
0.04	3.01			pH * rDOS/Aeration * Initial OD <sub>600nm</sub>
Prob > <i>F</i>	<i>F</i> -value	Prob > <i>F</i>	<i>F</i> -value	
0.09	4.28	<0.01	19.24	1st order
0.04	9.03			2nd order
0.06	142.89	0.86	0.3	Lack of fit
	0.7		0.89	Adjusted R <sup>2</sup>

**Table 4. DoE Output.** For each variable of the DoE, the *p*-value for a linear correlation (calculated via ANOVA), the *p*-value for the variables just at pH 8 (calculated via T-test) and the resulting outputs are stated.

Variable	<i>t</i> -Value (ANOVA)	<i>p</i> -Value (Data Points at pH 8)	Output
pH	<0.001	-	Optimum at pH 8
Aeration rate	0.29	0.17	Setpoint at 0.25 vvm as no significance detected
Initial OD <sub>600nm</sub>	0.41	0.46	Setpoint at 1 as no significance detected
rDOS	0.71	0.86	Setpoint set to 30% as no significant effect detected

With regards to the total carotenoids formed, a clear benefit of low pH and low rDOS is visible (Table 2). A model including the two-factor interaction between rDOS and pH, as well as the first-order components, showed a non-significant lack of fit (Prob > *F* of 0.06), while explaining 70% of the variability. Further two-factor interactions were omitted, as their inclusion only increased the lack of fit of the model. Overall, it was possible to increase the total carotenoid titer to 189.77 mg L<sup>−1</sup> at low pH, rDOS, aeration and initial OD<sub>600nm</sub>, while increasing initial OD<sub>600nm</sub> and aeration rate decreased this titer to 103.71 mg L<sup>−1</sup>. This is an up to 10-fold increase in total carotenoids in comparison to the control condition.

In regards to growth, a significant decrease in growth rates was observed at pH 6 (0.12 ± 0.02 h<sup>−1</sup>) compared to pH 8 (0.19 ± 0.03 h<sup>−1</sup>) (Table S1). The maximum CDW was also decreased at pH 6 (5.5 ± 1.4 g L<sup>−1</sup>) compared to pH 8 (9.4 ± 0.7 g L<sup>−1</sup>). However, the decrease was not significant due to run 8 showing a far higher maximum CDW than the other runs at pH 6.

Detailed information about the carotenoid titers under each condition are shown in Figure S1.

### 3.2. Validation of Optimal Batch Fermentation Conditions

#### 3.2.1. Further Analysis of the Influence of the Aeration Rate on Astaxanthin Production in Batch Cultivation

The ANOVA indicated no significant effect of the aeration rate on the astaxanthin titer among the tested conditions (Table 4). However, as the pH strongly affected the formation of xanthophylls and might have masked the effect of the aeration rate, we further investigated a potential influence of the aeration rate on the astaxanthin formation. Four batch fermentations were performed with aeration rates of 0.15, 0.25, 0.35 or 0.5 vvm (Figure 3A–D), and the other parameters were set as follows: rDOS at 30%, initial OD<sub>600nm</sub> of 1 and pH at 7.

The cultures with the lower aeration rates of 0.15 and 0.25 vvm grew to maximum OD<sub>600nm</sub> of 52 and 53 (12.9 to 13.4 g CDW L<sup>-1</sup>) with a growth rate of 0.25 and 0.26 h<sup>-1</sup>, respectively. At higher aeration rates of 0.35 and 0.5 vvm, the growth was slightly impaired, with respective growth rates of 0.20 and 0.22 h<sup>-1</sup> and maximum OD<sub>600nm</sub> of 42 and 46 (10.7 to 11.5 g CDW L<sup>-1</sup>).

At aeration rates of 0.15 and 0.35 vvm, 2.38 mg L<sup>-1</sup> and 2.14 mg L<sup>-1</sup> astaxanthin were produced, respectively, each corresponding to 0.24 mg g<sup>-1</sup> CDW. With an even higher aeration rate of 0.5 vvm, i.e., the control condition of the DoE runs, the astaxanthin production dropped to 0.93 mg L<sup>-1</sup> (0.11 mg g<sup>-1</sup> CDW). An aeration rate of 0.25 vvm led to the highest astaxanthin production of 5.53 mg L<sup>-1</sup> (0.61 mg g<sup>-1</sup> CDW), with a productivity of 0.12 mg g<sup>-1</sup> CDW h<sup>-1</sup> (Figure 3B). In comparison to the other aeration rates, the astaxanthin production was improved about 2–5-fold under these conditions.

To sum up, the aeration rate indeed had an impact on astaxanthin production, and optimal production was recorded at an aeration rate 0.25 vvm, as it was already indicated by the DoE approach. Accordingly, all further experiments were conducted with an aeration rate of 0.25 vvm.

#### 3.2.2. Validation of pH 8 as Setpoint for Optimal Astaxanthin Production in Batch Cultivation

The results of the DoE approach highlight the pH as the most important process parameter with regard to maximal astaxanthin titers. During the DoE fermentation runs, only integer pH setpoints were tested. Owing to the high significance of this variable, further detailed examination of the pH optimum with regard to astaxanthin production was performed.

Three identical batch fermentations were performed with varied pH setpoints of pH 7.5, 8 and 8.5 (Figure 3E–G). All other process parameters were kept constant, according to the DoE output (aeration rate of 0.25 vvm, 30% rDOS and an initial OD<sub>600nm</sub> of 1).

The culture at pH 7.5 grew to a maximal biomass concentration of 11.8 g CDW L<sup>-1</sup>, with a growth rate of 0.26 h<sup>-1</sup>. Growth was slightly impaired at pH 8, with a reduced growth rate of 0.21 h<sup>-1</sup> but a comparable biomass formation of 12.6 g CDW L<sup>-1</sup>. Cultivation at pH 8.5 led to a growth deficit, as the culture only grew to a maximal biomass concentration of 8.7 g CDW L<sup>-1</sup> with a reduced growth rate of 0.10 h<sup>-1</sup>. Lowering or increasing the pH setpoint to 7.5 or 8.5 resulted in lower astaxanthin production of 6.07 and 5.91 mg L<sup>-1</sup> (0.82 and 0.67 mg g<sup>-1</sup> CDW), respectively. Astaxanthin production, again, was highest at pH 8, with 7.12 mg L<sup>-1</sup> (0.81 mg g<sup>-1</sup> CDW) of astaxanthin corresponding to a volumetric productivity of 0.15 mg L<sup>-1</sup> h<sup>-1</sup> and a yield of 0.18 mg g<sup>-1</sup> glucose (Figure 3F).

Considering the total carotenoid production (Figure S2C,E–G), it becomes apparent that changes in the pH value do not only impact the astaxanthin production but also the precursor composition. At pH 7 and 7.5, mainly adonirubin and canthaxanthin accumulated, while at pH 8, lycopene and β-carotene were the predominant precursors being produced.

The cultivation under optimal conditions (pH 8, 0.25 vvm aeration rate, 30% rDOS, initial OD<sub>600nm</sub> of 1) was performed two additional times, adding up to technical triplicates (marked in green in Table S1) with an average astaxanthin titer of 7.61 ± 0.60 mg L<sup>-1</sup>.



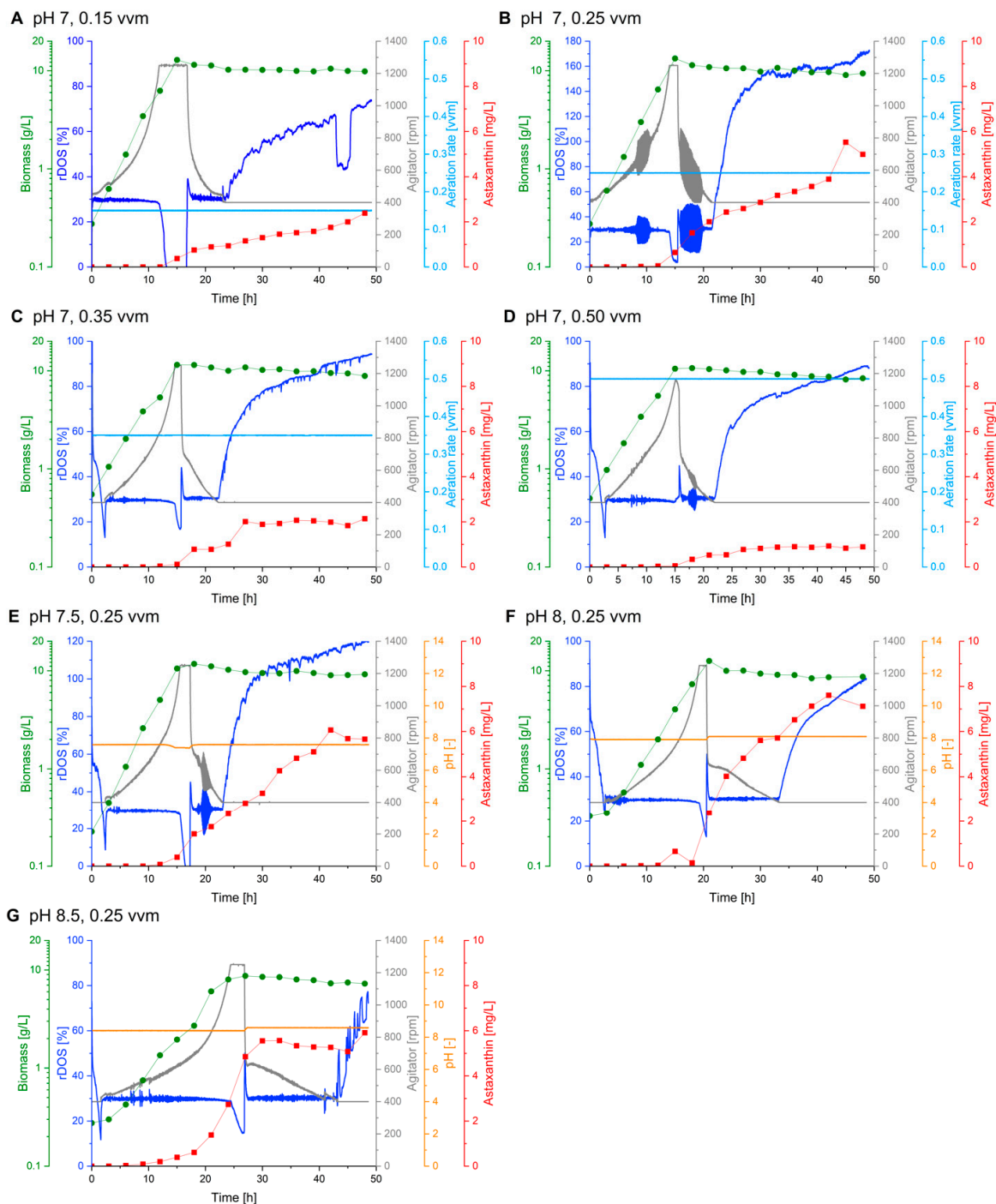


**Figure 3. Batch fermentations at different aeration rates and pH.** Astaxanthin titers (red squares), biomass (cell dry weight; green dots), agitator speed (grey line), rDOS (dark blue line), aeration rate (light blue line) and pH (orange line) over time during batch fermentations with *C. glutamicum* ASTA\* grown in 2 L CGXII medium at pH 7 with an aeration rate of 0.15 vvm (A), 0.25 vvm (B), 0.35 vvm (C) or 0.5 vvm (D); or with an aeration rate of 0.25 vvm at pH 7.5 (E), pH 8 (F) or pH 8.5 (G). All fermentations were performed with an initial OD<sub>600nm</sub> of 1, at rDOS of 30%.

### 3.2.3. pH-Shift Experiments in Late Exponential Phase Indicate Different pH Optima for Astaxanthin Biosynthesis and Its Precursor Biosynthesis

The DoE results demonstrated that astaxanthin production possesses a pH optimum of 8 (Figures 2 and 3A–D). In contrast, the precursor  $\beta$ -carotene accumulates to high titers

of up to  $127 \text{ mg L}^{-1}$  at pH 6 (Figure S1). This indicated that at pH 6 oxy-functionalization to astaxanthin by CrtZ and CrtW is a bottleneck. It was tested whether a two-stage production process starting with a  $\beta$ -carotene accumulating phase at pH 6 followed by a second phase with a pH shift to 8 for conversion to astaxanthin (pH 6 $\rightarrow$ 8) is beneficial in comparison to a one-stage bioprocess. Vice versa, a pH-shift fermentation was performed starting at pH 8, with a shift to pH 6 at 12 h after inoculation (pH 8 $\rightarrow$ 6) (Figure 4B,D, respectively). For comparison, two batch cultivations with a constant pH of 6 or 8 were performed (Figure 4A,C, respectively). All four fermentations were carried out at optimal setpoints (aeration rate of 0.25 vvm, 30% rDOS and initial  $\text{OD}_{600\text{nm}}$  of 1) (Figure 4). The fermentation with constant pH 6 showed strongly impaired growth, with a maximum biomass formation of  $2.65 \text{ g CDW L}^{-1}$  and a reduced growth rate of  $0.12 \text{ h}^{-1}$ . Instead, at pH 8, the culture grew to a maximum biomass concentration of  $14.25 \text{ g CDW L}^{-1}$  with a growth rate of  $0.24 \text{ h}^{-1}$ . In comparison, both fermentations with a pH-shift (pH6 $\rightarrow$ 8, pH8 $\rightarrow$ 6) exhibited slight growth deficits with maximal biomass formation of 10.3 or  $11.7 \text{ g CDW L}^{-1}$  and growth rates of 0.21 and  $0.23 \text{ h}^{-1}$ , respectively. Analysis of the carotenoids revealed that during the fermentation with a constant pH 6, only  $0.04 \text{ mg L}^{-1}$  ( $0.04 \text{ mg g}^{-1} \text{ CDW}$ ) of astaxanthin was produced, while  $\beta$ -carotene accumulated to  $18.26 \text{ mg L}^{-1}$  ( $7.16 \text{ mg g}^{-1} \text{ CDW}$ ) (Figure 4A).

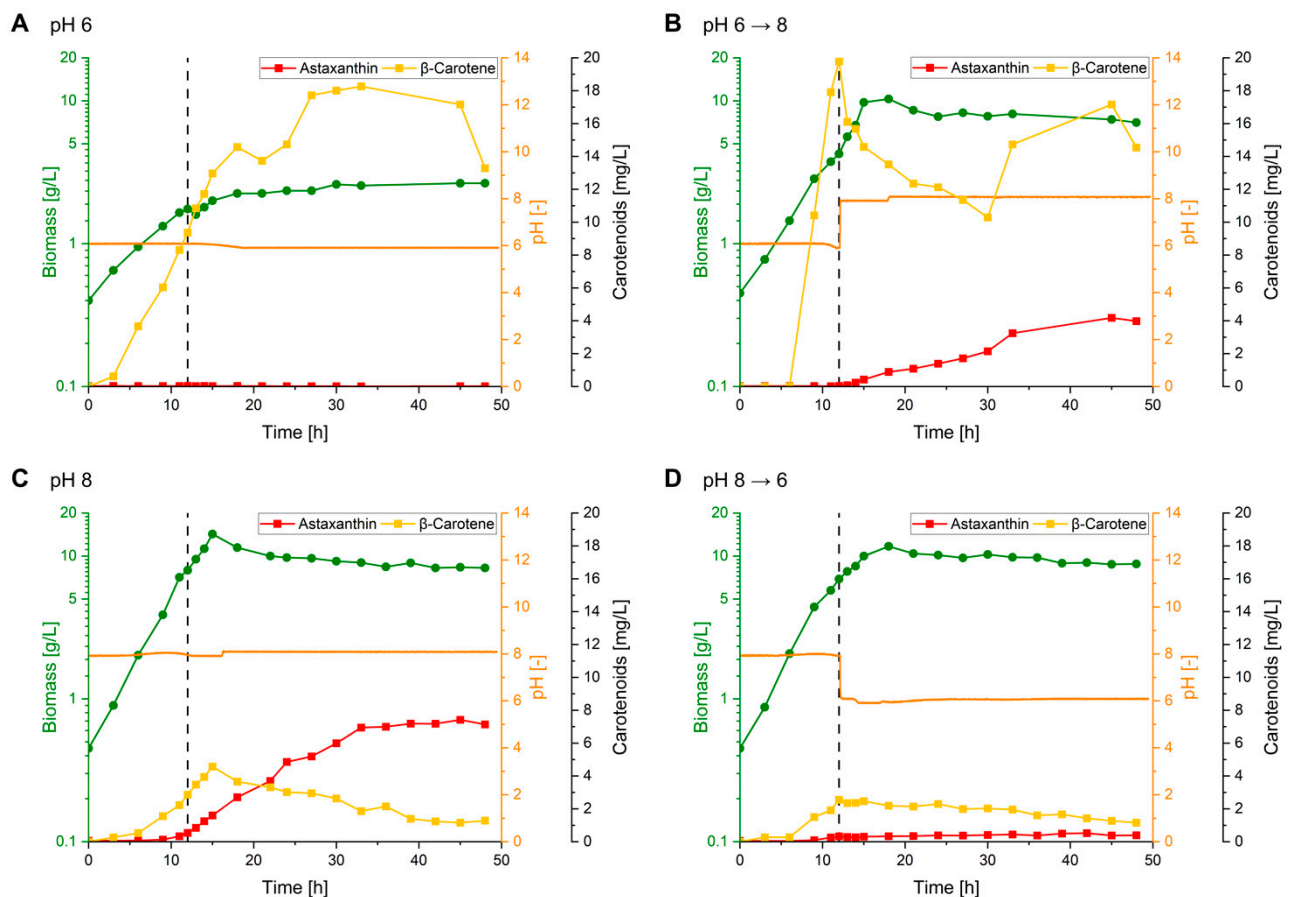


**Figure 4. Batch fermentations for pH-shift experiments.** Astaxanthin titer (red squares),  $\beta$ -carotene titer (yellow squares), biomass (cell dry weight; green dots) and pH (orange line) over time during batch fermentations with *C. glutamicum* ASTA\* grown in 2 L CGXII medium steady at pH 6 (A), pH 8 (B) or with a pH shift after 12 h from pH 6 to pH 8 (C) or from pH 8 to pH 6 (D). All fermentations were performed with an initial  $\text{OD}_{600\text{nm}}$  of 1, at rDOS of 30% and an aeration rate of 0.25 vvm.

In the fermentation with a pH-shift from 8 to 6, astaxanthin was mainly produced during the first phase at pH 8 (Figure 4D). Here,  $0.33 \text{ mg L}^{-1}$  ( $0.05 \text{ mg g}^{-1} \text{ CDW}$ ) of astaxanthin accumulated, which is comparable to the fermentation with constant pH of 8 at 12 h after inoculation ( $0.53 \text{ mg L}^{-1}$  ( $0.07 \text{ mg g}^{-1} \text{ CDW}$ )) 12 h (Figure 4C). In the second phase after the pH shift to 6, the astaxanthin content remained low, with a maximum production of  $0.52 \text{ mg L}^{-1}$  ( $0.12 \text{ mg g}^{-1} \text{ CDW}$ ). Remarkably,  $\beta$ -carotene also only accumulated during the first phase at pH 8 to a maximum titer of  $2.55 \text{ mg L}^{-1}$  ( $0.37 \text{ mg g}^{-1} \text{ CDW}$ ), whereas  $\beta$ -carotene levels were slowly decreasing in the second phase.

In the two-stage bioprocess with a pH-shift from 6 to 8, no astaxanthin accumulated in the first phase, but in the second phase up to  $4.18 \text{ mg L}^{-1}$  ( $0.57 \text{ mg g}^{-1} \text{ CDW}$ ) of astaxanthin was produced (Figure 4B). Prior to the pH-shift,  $\beta$ -carotene production was strong, and titers comparable to the cultivation with a continuous pH of 6 were reached ( $19.78 \text{ mg L}^{-1}$  or  $4.65 \text{ mg g}^{-1} \text{ CDW}$ ). In the second phase with pH 8,  $\beta$ -carotene was converted to astaxanthin until it started to accumulate again after 30 h of cultivation. It is noteworthy that after the shift from pH 6 to 8, adonirubin and canthaxanthin started to accumulate, while  $\beta$ -carotene remained the most abundant precursor (Figures S3 and S4). During the fermentation at continuous pH 8,  $7.42 \text{ mg L}^{-1}$  ( $0.89 \text{ mg g}^{-1} \text{ CDW}$ ) astaxanthin accumulated, with a productivity of  $0.15 \text{ mg L}^{-1} \text{ h}^{-1}$ , while  $\beta$ -carotene production remained low (max.  $4.57 \text{ mg L}^{-1}$  or  $0.32 \text{ mg g}^{-1} \text{ CDW}$ ) (Figure 4C).

In summary, a two-stage bioprocess with pH-shift (pH 6→8) for (i) initial precursor accumulation and (ii) subsequent conversion to astaxanthin did not increase astaxanthin production. Thus, a one-stage bioprocess with constant pH 8 remains optimal for astaxanthin production.

### 3.3. Transfer of Optimized Batch Bioprocess Conditions to Fed-Batch Bioprocess Accelerated Astaxanthin Production

The optimal conditions for astaxanthin production under batch conditions were transferred to a fed-batch bioprocess. Previously, we used a CGXII-based feed solution, and while we observed satisfying growth behavior, astaxanthin production was lower than in the best batch fermentations shown here. Additionally, the feed solution showed solubility problems due to high concentrations of phosphate, calcium and magnesium salts [34]. To combat these problems, we switched to an established minimal salts HCDC batch medium developed for *C. glutamicum* [39] with  $600 \text{ g L}^{-1}$  glucose as feed solution.

Two fed-batch cultivations were performed in parallel, comparing the initial setpoints (0.5 vvm, pH 7) with the optimized batch cultivation conditions (0.25 vvm, pH 8 (Figure 5). Over the course of the process, the initial aeration rate was increased manually, to prevent oxygen starvation with increasing cell densities.

Both cultures grew with comparable growth rates of  $0.15$  and  $0.13 \text{ h}^{-1}$  to a maximal biomass concentration of  $98$  and  $60 \text{ g CDW L}^{-1}$  at pH 7 and 8, respectively. In the fermentation at pH 7,  $55 \text{ mg L}^{-1}$  astaxanthin ( $0.68 \text{ mg g}^{-1} \text{ CDW}$ ) was produced with a volumetric productivity of  $0.73 \text{ mg L}^{-1} \text{ h}^{-1}$  and a yield of  $0.18 \text{ mg g}^{-1}$  glucose (Figure 5A). Astaxanthin production at pH 8 surpassed production at pH 7 in all cases. During the fed-batch fermentation at pH 8,  $64 \text{ mg L}^{-1}$  astaxanthin ( $1.22 \text{ mg g}^{-1} \text{ CDW}$ ) was produced with a volumetric productivity of  $0.85 \text{ mg L}^{-1} \text{ h}^{-1}$  and a yield of  $0.21 \text{ mg g}^{-1}$  glucose (Figure 5B).

Considering the total carotenoid output during the fed-batch processes, it can be stated that during both fermentations comparable total carotenoid amounts in astaxanthin equivalents were produced ( $333 \text{ mg L}^{-1}$  at pH 7 and  $317 \text{ mg L}^{-1}$  at pH 8) (Figure S5). Yet, it is remarkable that, at pH 7, mostly the direct astaxanthin precursor adonirubin and canthaxanthin accumulated to high amounts ( $102$  and  $99 \text{ mg L}^{-1}$ , respectively), while at pH 8 these precursors were mostly converted to astaxanthin. Instead, the earlier precursors lycopene and  $\beta$ -carotene accumulated ( $93$  and  $94 \text{ mg L}^{-1}$ , respectively) during the process at pH 8.

In conclusion, the fed-batch fermentation at pH 8 resulted in the highest astaxanthin titer of 64 mg L<sup>-1</sup>, which corresponds to an about 9-fold improvement in comparison to the optimized batch process.

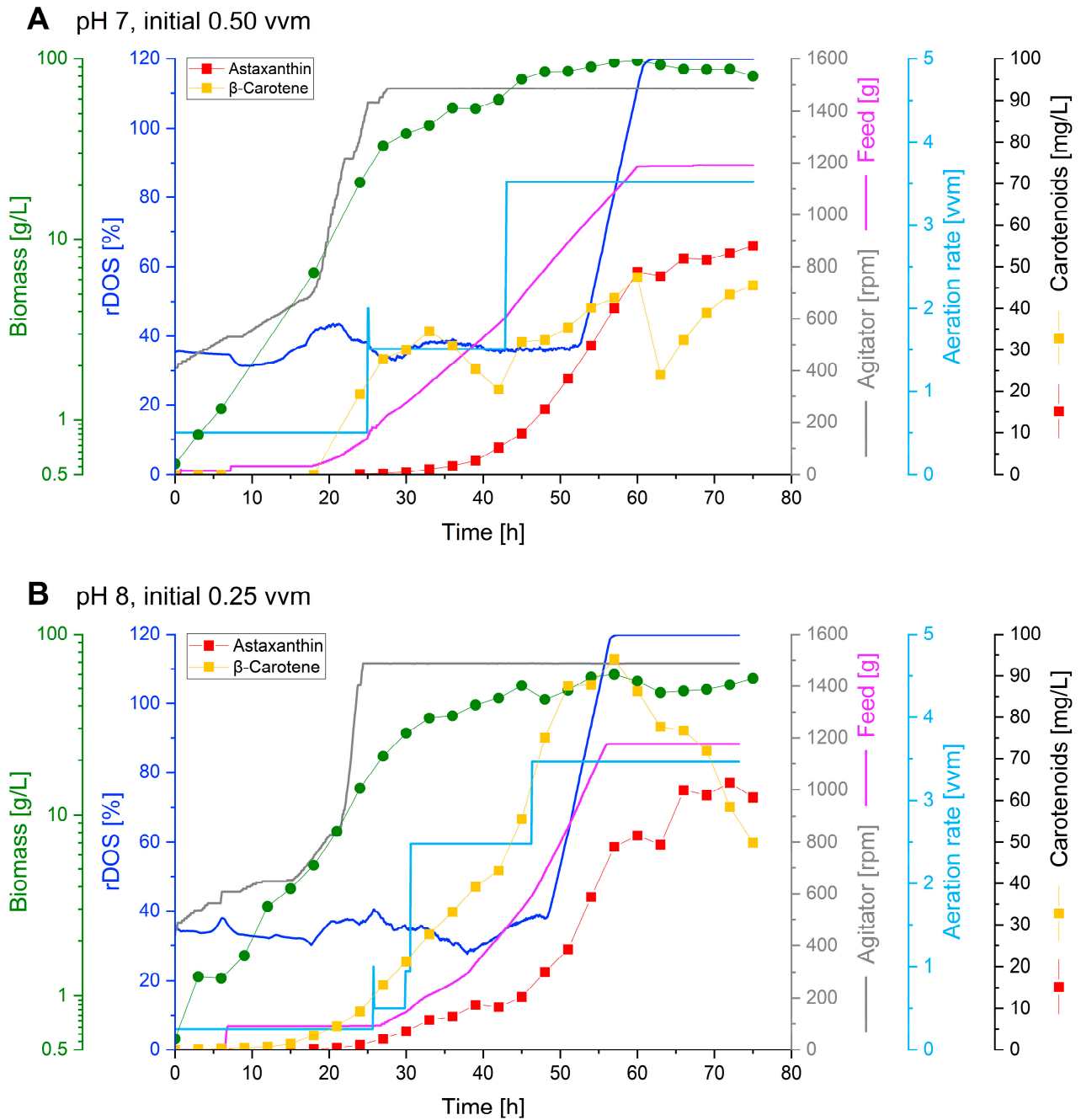


**Figure 5. Fed-batch fermentations.** Astaxanthin titers (red squares),  $\beta$ -carotene titers (yellow squares), biomass (cell dry weight; green dots), feed intake (purple line), agitator speed (grey line), moving average rDOS (dark blue line), and aeration rate (light blue line) over time during fed-batch fermentations with *C. glutamicum* ASTA\* grown in 1 L HCDC as batch medium, fed with 1 L 600 g L<sup>-1</sup> glucose at pH 7 with an initial aeration rate of 0.5 vvm (A) or at pH 8 with an initial aeration rate of 0.25 vvm (B).

#### 4. Discussion

Fermentative astaxanthin production with *C. glutamicum* was improved in a DoE-guided approach with regard to the process setpoints pH, aeration rate, rDOS and initial optical density in batch and fed-batch mode. The parameter optimization effect was stronger in batch mode (approximately 4-fold improvement compared to control conditions) than it was in fed-batch mode (approximately 1.2-fold improvement). Compared to the improved batch process, the astaxanthin product titer increased about 9-fold, from 7 mg L<sup>-1</sup> to 64 mg L<sup>-1</sup> in fed-batch fermentation. The more than 4-fold increased maximal biomass formation and the increased astaxanthin content (0.87 to 1.2 mg g<sup>-1</sup> CDW) contributed to the improvement. The volumetric productivity improved approx. 6-fold from 0.15 mg L<sup>-1</sup> h<sup>-1</sup> in batch conditions to 0.86 mg L<sup>-1</sup> h<sup>-1</sup> in the fed-batch process, while the yield was increased by about 10% (0.18 and 0.21 mg g<sup>-1</sup> glucose, respectively). Thus, these three key performance indicators of the high cell density astaxanthin bioprocess could be improved by the described process intensification.

In this study, we identified pH as the predominant process parameter to influence growth and carotenoid production of *C. glutamicum*. *C. glutamicum* can effectively maintain an intracellular pH of 7.5 ± 0.5 when exposed to external pH values between pH 5.5 and pH 9 [46,52,53]. However, sharp differences were determined in growth and carotenoid production between pH 6, 7 and 8, with the latter pH being the optimum for astaxanthin production. pH 6 was best for accumulation of the carotenogenic precursor β-carotene, whereas both growth rates as well as final biomass titer were reduced. This growth deficiency may be explained with higher oxidative stress at pH 6 in comparison to pH 7.5 or 9 [46]. In contrast, higher oxidative stress levels have been shown to influence carotenoid biosynthesis positively in *E. coli* [54]. Although we did not observe any byproduct formation at pH 6 (data not shown) that could explain a reduced biomass formation, as seen in a previous research study with pyruvate accumulation under cultivation at pH 6 [46], it is tempting to speculate that increased pyruvate availability could boost the methylerythritol phosphate pathway, as it serves as its substrate, together with GAP. Indeed, pH 6 was found to be the most beneficial for total carotenoid production in this study. The previously observed feedback inhibition from xanthophylls on their precursors [31] likely also plays a role here and could explain the increase in total carotenoids due to the absence of xanthophylls.

NADPH availability was previously identified as a potential bottleneck in carotenoid production with *C. glutamicum* in BioLector<sup>®</sup> cultivations at pH 7 [32]. Furthermore, it was reported that the NADP<sup>+</sup>/NADPH concentrations are reduced by 50% in *C. glutamicum* during bioreactor cultivations at pH 6 [46]. These data cannot explain the observations in this study, as the highest total carotenoid (primarily β-carotene) concentrations were measured at pH 6. However, xanthophyll, especially astaxanthin, production was almost fully inhibited at pH 6 and maximal at pH 8. As β-carotene biosynthesis from glucose requires 16 NADPH either directly or transferred via ferredoxin, while terminal astaxanthin biosynthesis from β-carotene requires only six additional reduction equivalents, a limitation in reduction equivalents is not a likely explanation for the inhibited astaxanthin production. pH-shift fermentations suggested that the conversion towards astaxanthin was abolished at pH 6 but that biosynthesis could be quickly restored after the pH shift to 8. The enzyme CrtZ~W represents a translational fusion of the β-carotene hydroxylase (CrtZ) and β-carotene ketolase (CrtW) from the marine bacterium *F. pelagi* [55]. For the xylose isomerase (XI) from *F. pelagi* it was shown that it exhibits its maximum catalytic activity in a pH range from 6.3 to greater than 7.8, while the activity decreased by 70% at pH 6 [56], corresponding to the alkaline conditions of the ocean with a pH of 8.1 [57]. To the best of our knowledge, no enzyme assay data are available for the Crt enzymes of *F. pelagi*. *In vitro* assays for other CrtZ and CrtW proofed enzyme activities at pH 8 [58] and pH 7.6 [59] but without the determination of the pH optima.



A comparison of the pH optimum for astaxanthin production is not trivial between different hosts, but it can be summarized that processes have been performed at neutral pH 7.2 for *P. carotinifaciens* [60] or pH 7 for *E. coli* [61,62] and *Haematococcus pluvialis* [63] or at acidic pH, e.g., with yeasts *Y. lipolytica* [16] and *S. cerevisiae* [17] at pH 5.5 and 5.8, respectively. The identification of an alkaline pH as optimal for astaxanthin formation is a novelty within this study.

Two other important physical parameters, namely aeration rate and rDOS setpoint controlled via agitation, were identified in this study, showing a clear effect on total carotenoid formation at low pH. Additionally, we could later also show that the aeration rate in fact has an effect on astaxanthin formation.

Sufficient oxygen supply is essential for aerobic organisms like *C. glutamicum* and is influenced by aeration and agitation as bioprocess parameters. However, changing these parameters does not only affect oxygen but also CO<sub>2</sub> levels in the fermentation [64–66]. As was shown in the initial set of batch fermentations, both aeration and agitation strongly influence the total carotenoid content of the cells, albeit only at pH 6. This low pH further supports the effect being caused by the pCO<sub>2</sub> as it moves the reaction balance towards gaseous CO<sub>2</sub> and therefore eases off gassing. In addition, changes in aeration rate should only influence CO<sub>2</sub> levels, as the rDOS is kept constant by changing the stirring rate. This is further supported by changes in off-gas CO<sub>2</sub> concentrations we measured. Increasing the rDOS setpoint from 15% to 30% almost doubled the average off-gas CO<sub>2</sub> from 1.6 to 3.5%, while increasing aeration increased it from 2.2 to 3% (Figure S6). At higher pH, a positive effect is still visible; however, here we observed an increase in the transformation of β-carotene and intermediates into astaxanthin.

Several studies have focused on the effects of CO<sub>2</sub> on *C. glutamicum* [67–69]. Low CO<sub>2</sub> concentrations have been shown to increase the thiamine production that represents a competing pathway to the MEP pathway and therefore might reduce carotenoid production. An increased thiamin concentration enables a higher flux through the pyruvate dehydrogenase complex and pyruvate:quinone oxidoreductase that could potentially reduce the available pool of pyruvate and GAP for the MEP pathway [69]. A reduced biomass per substrate yield was observed under low CO<sub>2</sub> conditions, whereas under high CO<sub>2</sub> conditions Blombach et al. observed increased biomass per substrate yields, likely due to changes in the anaplerotic node of *C. glutamicum* [69]. Correspondingly, in this study a declining biomass formation was observed at pH 6, when combined with high aeration and rDOS, which supports the hypothesis that these effects are primarily pCO<sub>2</sub>-caused. This might explain both the benefits for total carotenoid as well as astaxanthin production that we observed under low aeration and agitation [69].

Moreover, Blombach et al. 2013 observed a differential expression of the DtxR regulon under high CO<sub>2</sub> concentrations, indicating an increased availability of reduced iron and subsequently a reduced expression of genes involved in iron uptake [69]. Another study showed that CO<sub>2</sub> plays a direct role in the reduction of iron in complexes with PCA or other phenolic compounds [70]. It is tempting to speculate that an increase in reduced iron caused by the low aeration rate has a positive effect on the iron-dependent enzymes CrtZ and CrtW from astaxanthin biosynthesis [58]. It can be hypothesized that the positive effects from the low aeration are based on an increased availability of reduced iron. This is further supported by the inhibition of xanthophyll synthesis at a low pH, as it has been previously shown that a low pH induces the iron-starvation response in *C. glutamicum* [46]. As such, both effects combined could explain the complete absence of astaxanthin at low pH while aeration and rDOS are high.

Under low CO<sub>2</sub> conditions, it was shown that the ferredoxin gene *cysX* (cg3117/WP\_011266012.1) and the ferredoxin reductase gene *fpr2* (cg3119/WP\_011015406.1) were significantly downregulated [69]. Both the β-carotene hydroxylase CrtZ [59] as well as several steps in the MEP pathway (e.g., IspG [71]) are ferredoxin-dependent and could be negatively impacted [29]. While CysX and Fpr2 have been shown to be important for sulfur assimilation, their effect on carotenoid biosynthesis is unknown in *C. glutamicum* [72].

In addition, altered levels of CO<sub>2</sub> could directly change the membrane fluidity [67,73]. Different CO<sub>2</sub> concentrations were shown to result in differentially expressed genes encoding for membrane proteins that could lead to changes in membrane fluidity [69]. In fact, it is well known that carotenoids influence membrane fluidity and their biosynthesis could therefore also be sensitive to membrane changes [74]. As membrane engineering has been demonstrated as a strategy for enhanced carotenoid production [75], the possible effect of CO<sub>2</sub> on membrane fluidity is interesting for future research. Although most of the membrane proteins are of unknown function [69], similar observations have been made in *P. aeruginosa* [76] and many other organisms [77].

Our previous work on astaxanthin production with *C. glutamicum* ASTA\* presented a batch fermentation in CGXII medium at pH 7 with an aeration rate of 0.5 vvm, rDOS of 30% and an initial OD<sub>600nm</sub> of 2 [34], achieving an astaxanthin titer of 3.12 mg L<sup>-1</sup> [34]. With the here-presented optimized process parameters the astaxanthin titer was more than doubled.

Our previous fed-batch attempt with *C. glutamicum* ASTA\* was performed in CGXII supplemented with an aquaculture sidestream as batch and a CGXII concentrate as feed [34]. This led to a 3.5-fold increase in biomass formation compared to batch conditions, while the astaxanthin titer only increased 1.3-fold (6 mg L<sup>-1</sup>) [34]. Here, biomass and astaxanthin titers were improved 4-fold and 9-fold, respectively, by fed-batch fermentation, indicating the superiority of the HCDC medium. The HCDC medium has proven to result in biomass titers of 227 g L<sup>-1</sup> CDW based on a 900 g L<sup>-1</sup> glucose feed [39], suggesting that astaxanthin production may be further improved with higher glucose concentration in the feed.

Our previous studies on the metabolic engineering of *C. glutamicum* for astaxanthin indicated that a feedback regulation of the lycopene β-cyclase or further upstream in the carotenoid biosynthetic pathway might limit the overall production [21,31]. This phenomenon is widely described in literature for other microbial hosts such as *H. pluvialis* [78] and *E. coli* [20]. As this feedback inhibition has not yet been solved with metabolic engineering strategies, a two-stage bioprocess for optimized precursor and terminal biosynthesis might tackle the challenges of feedback inhibition. The pH-shift experiments in this study revealed that a two-stage bioprocess to tackle the feedback inhibition in the astaxanthin biosynthesis [31] and to decouple precursor and production formation was not beneficial under the tested batch conditions. It is noteworthy that, after the pH shift from pH 6 to 8, adonirubin and canthaxanthin started to accumulate, while β-carotene remained the most abundant precursor. This indicates that CrtW and CrtZ remain bottlenecks after the pH shift in the presented batch process, as β-carotene was only partially converted into astaxanthin. In summary, a constant pH 8 remains the optimal condition for astaxanthin production in batch mode so far. A two-stage process might still be beneficial in a fed-batch mode when considering all process parameters to be adapted for an optimized precursor production, namely β-carotene, during the first stage of the bioprocess.

Astaxanthin production by *P. rhodozyma* was optimized in shake flasks with temperature and carbon concentration as the most impactful process parameters [79]. Accordingly, the cultivation temperature could be optimized for the here-presented process for all fermentations in this study at 30 °C as the standard temperature for *C. glutamicum* [48]. Furthermore, optimization of the initial carbon concentration, as well as an adapted feed protocol for the fed-batch fermentations, may be beneficial. As the current feed protocol relies on recurring carbon starvation, a feed profile which is optimized for a steady carbon concentration or is adapted for exponential growth may be advantageous for product formation [80–82].

In this study, astaxanthin production by *C. glutamicum* was successfully transferred from shake-flask cultivation to stirred tank batch and fed-batch processes. In regard to an industrial application, a repeated fed-batch or a continuous process strategy may be applied [83]. Both strategies allow for high cell densities [84–86] and are designed for frequent or continuous product output, respectively. Furthermore, the current production volume of 2 L would need to be enlarged for an industrial application. A traditional way to scale up biotechnological processes is to choose one scale-up criterion like the oxygen

volumetric mass transfer coefficient ( $k_L a$ ) or the power input per unit volume (P/V) and keep them constant throughout larger scales [87]. From this point of view, the transfer to a continuous process could be one strategy to optimize P/V at a small scale and later use it as criterion for scale-up.

**Supplementary Materials:** The following supporting information can be downloaded at: <https://www.mdpi.com/article/10.3390/fermentation9110969/s1>, Figure S1: Carotenoid titers of *C. glutamicum* ASTA\* at the time of maximum astaxanthin titer of each DoE run. Figure S2: Carotenoid titers and biomass formation of *C. glutamicum* ASTA\* during batch fermentations at different aeration rates and pH. Figure S3: Carotenoids titers and biomass formation of *C. glutamicum* ASTA\* during batch fermentations at different pH values and with pH-shifts. Figure S4: Cellular carotenoid contents of *C. glutamicum* ASTA\* during fermentations at different pH values and with pH-shifts. Figure S5: Carotenoid titers and biomass formation of *C. glutamicum* ASTA\* during fed-batch fermentations. Figure S6: Off-gas CO<sub>2</sub> profiles of the batch DoE fermentation runs 1–10. Table S1: Fermentation parameters, astaxanthin production and growth indicators.

**Author Contributions:** Conceptualization, F.M., I.S., V.F.W. and N.A.H.; investigation, F.M. and I.S.; resources: T.S.; writing—original draft preparation, I.S. and F.M.; writing—review and editing, V.F.W. and N.A.H.; supervision, V.F.W. and N.A.H.; project administration, N.A.H.; funding acquisition, V.F.W. and N.A.H. All authors have read and agreed to the published version of the manuscript.

**Funding:** This research was funded by the German Federal Ministry of Education and Research (BMBF) project KaroTec (grant number: 03VP09460). IS, FM, and NAH acknowledge funding by the ERA CoBlueBio project SIDESTREAM cofunded by the BMBF (grant number: 161B0950A). Support for the article processing charge by the Deutsche Forschungsgemeinschaft and the Open Access Publication Fund of Bielefeld University is acknowledged. The funding bodies had no role in the design of the study or the collection, analysis, or interpretation of data, or in writing the manuscript.

**Institutional Review Board Statement:** Not applicable.

**Informed Consent Statement:** Not applicable.

**Data Availability Statement:** All data are presented in the manuscript and its supplementary material.

**Acknowledgments:** We thank Joe Max Risse from the Fermentation Technology, Technical Faculty and CeBiTec, Bielefeld University, for technical assistance and advice. Furthermore, we thank Petra Peters-Wendisch from the Institute for Genetics of Prokaryotes, Faculty of Biology and CeBiTec, Bielefeld University for scientific discussion. Additionally, we thank Alina Witt for assistance during the DoE fermentation runs and Charlotte Bramers for assistance with preliminary fermentation tests.

**Conflicts of Interest:** The authors declare no conflict of interest.

## References

1. Naguib, Y.M.A. Antioxidant Activities of Astaxanthin and Related Carotenoids. *J. Agric. Food Chem.* **2000**, *48*, 1150–1154. [[CrossRef](#)] [[PubMed](#)]
2. Dose, J.; Matsugo, S.; Yokokawa, H.; Koshida, Y.; Okazaki, S.; Seidel, U.; Eggersdorfer, M.; Rimbach, G.; Esatbeyoglu, T. Free Radical Scavenging and Cellular Antioxidant Properties of Astaxanthin. *Int. J. Mol. Sci.* **2016**, *17*, 10103. [[CrossRef](#)] [[PubMed](#)]
3. Pereira da Costa, D.; Campos Miranda-Filho, K. The Use of Carotenoid Pigments as Food Additives for Aquatic Organisms and Their Functional Roles. *Rev. Aquac.* **2020**, *12*, 1567–1578. [[CrossRef](#)]
4. Zhang, L.; Wang, H. Multiple Mechanisms of Anti-Cancer Effects Exerted by Astaxanthin. *Mar. Drugs* **2015**, *13*, 4310–4330. [[CrossRef](#)] [[PubMed](#)]
5. Chang, M.X.; Xiong, F. Astaxanthin and Its Effects in Inflammatory Responses and Inflammation-Associated Diseases: Recent Advances and Future Directions. *Molecules* **2020**, *25*, 5342. [[CrossRef](#)]
6. Giannaccare, G.; Pellegrini, M.; Senni, C.; Bernabei, F.; Scorcia, V.; Cicero, A.F.G. Clinical Applications of Astaxanthin in the Treatment of Ocular Diseases: Emerging Insights. *Mar. Drugs* **2020**, *18*, 239. [[CrossRef](#)]
7. Pereira, C.P.M.; Souza, A.C.R.; Vasconcelos, A.R.; Prado, P.S.; Name, J.J. Antioxidant and Anti-inflammatory Mechanisms of Action of Astaxanthin in Cardiovascular Diseases (Review). *Int. J. Mol. Med.* **2021**, *47*, 37–48. [[CrossRef](#)]
8. Li, J.; Guo, C.; Wu, J. Astaxanthin in Liver Health and Disease: A Potential Therapeutic Agent. *Drug Des. Dev. Ther.* **2020**, *14*, 2275–2285. [[CrossRef](#)]
9. Oliyaei, N.; Moosavi-Nasab, M.; Tanideh, N.; Iraj, A. Multiple Roles of Fucoxanthin and Astaxanthin against Alzheimer's Disease: Their Pharmacological Potential and Therapeutic Insights. *Brain Res. Bull.* **2023**, *193*, 11–21. [[CrossRef](#)]

10. Shen, D.-F.; Qi, H.-P.; Ma, C.; Chang, M.-X.; Zhang, W.-N.; Song, R.-R. Astaxanthin Suppresses Endoplasmic Reticulum Stress and Protects against Neuron Damage in Parkinson's Disease by Regulating miR-7/SNCA Axis. *Neurosci. Res.* **2021**, *165*, 51–60. [CrossRef]
11. Grand-View-Research Astaxanthin Market Size, Share & Trends Analysis Report By Product (Oil, Softgel, Liquid), By Source (Natural, Synthetic), By Application (Aquaculture & Animal Feed, Nutraceuticals), By Region, And Segment Forecasts, 2021–2028. 2021. Available online: <https://www.grandviewresearch.com/industry-analysis/global-astaxanthin-market> (accessed on 2 June 2023).
12. Lim, K.C.; Yusoff, F.M.; Shariff, M.; Kamarudin, M.S. Astaxanthin as Feed Supplement in Aquatic Animals. *Rev. Aquac.* **2018**, *10*, 738–773. [CrossRef]
13. Butler, T.; Golan, Y. Astaxanthin Production from Microalgae. In *Microalgae Biotechnology for Food, Health and High Value Products*; Alam, M.A., Xu, J.-L., Wang, Z., Eds.; Springer: Singapore, 2020; pp. 175–242, ISBN 9789811501692.
14. Stachowiak, B.; Szulc, P. Astaxanthin for the Food Industry. *Molecules* **2021**, *26*, 2666. [CrossRef] [PubMed]
15. Ma, Y.; Li, J.; Huang, S.; Stephanopoulos, G. Targeting Pathway Expression to Subcellular Organelles Improves Astaxanthin Synthesis in *Yarrowia lipolytica*. *Metab. Eng.* **2021**, *68*, 152–161. [CrossRef]
16. Tramontin, L.R.R.; Kildegaard, K.R.; Sudarsan, S.; Borodina, I. Enhancement of Astaxanthin Biosynthesis in Oleaginous Yeast *Yarrowia lipolytica* via Microalgal Pathway. *Microorganisms* **2019**, *7*, 472. [CrossRef] [PubMed]
17. Jiang, G.; Yang, Z.; Wang, Y.; Yao, M.; Chen, Y.; Xiao, W.; Yuan, Y. Enhanced Astaxanthin Production in Yeast via Combined Mutagenesis and Evolution. *Biochem. Eng. J.* **2020**, *156*, 107519. [CrossRef]
18. Hayashi, M.; Ishibashi, T.; Kuwahara, D.; Hirasawa, K. Commercial Production of Astaxanthin with *Paracoccus carotinifaciens*. In *Carotenoids: Biosynthetic and Biofunctional Approaches*; Misawa, N., Ed.; Advances in Experimental Medicine and Biology; Springer: Singapore, 2021; pp. 11–20, ISBN 9789811573606.
19. Park, S.Y.; Binkley, R.M.; Kim, W.J.; Lee, M.H.; Lee, S.Y. Metabolic Engineering of *Escherichia coli* for High-Level Astaxanthin Production with High Productivity. *Metab. Eng.* **2018**, *49*, 105–115. [CrossRef] [PubMed]
20. Zhang, C.; Seow, V.Y.; Chen, X.; Too, H.-P. Multidimensional Heuristic Process for High-Yield Production of Astaxanthin and Fragrance Molecules in *Escherichia coli*. *Nat. Commun.* **2018**, *9*, 1858. [CrossRef]
21. Henke, N.A.; Wendisch, V.F. Improved Astaxanthin Production with *Corynebacterium glutamicum* by Application of a Membrane Fusion Protein. *Mar. Drugs* **2019**, *17*, 621. [CrossRef]
22. Seeger, J.; Wendisch, V.F.; Henke, N.A. Extraction and Purification of Highly Active Astaxanthin from *Corynebacterium glutamicum* Fermentation Broth. *Mar. Drugs* **2023**, *21*, 530. [CrossRef]
23. Krubasik, P.; Takaichi, S.; Maoka, T.; Kobayashi, M.; Masamoto, K.; Sandmann, G. Detailed Biosynthetic Pathway to Decaprenoxanthin Diglucoside in *Corynebacterium glutamicum* and Identification of Novel Intermediates. *Arch. Microbiol.* **2001**, *176*, 217–223. [CrossRef]
24. Li, C.; Swofford, C.A.; Rückert, C.; Chatzivasileiou, A.O.; Ou, R.W.; Opdensteinen, P.; Luttermann, T.; Zhou, K.; Stephanopoulos, G.; Jones Prather, K.L.; et al. Heterologous Production of  $\alpha$ -Carotene in *Corynebacterium glutamicum* Using a Multi-Copy Chromosomal Integration Method. *Bioresour. Technol.* **2021**, *341*, 125782. [CrossRef] [PubMed]
25. Henke, N.A.; Heider, S.A.E.; Hannibal, S.; Wendisch, V.F.; Peters-Wendisch, P. Isoprenoid Pyrophosphate-Dependent Transcriptional Regulation of Carotenogenesis in *Corynebacterium glutamicum*. *Front. Microbiol.* **2017**, *8*, 633. [CrossRef] [PubMed]
26. Henke, N.A.; Heider, S.; Peters-Wendisch, P.; Wendisch, V. Production of the Marine Carotenoid Astaxanthin by Metabolically Engineered *Corynebacterium glutamicum*. *Mar. Drugs* **2016**, *14*, 124. [CrossRef] [PubMed]
27. Kang, M.-K.; Eom, J.-H.; Kim, Y.; Um, Y.; Woo, H.M. Biosynthesis of Pinene from Glucose Using Metabolically-Engineered *Corynebacterium glutamicum*. *Biotechnol. Lett.* **2014**, *36*, 2069–2077. [CrossRef]
28. Ravikumar, S.; Woo, H.M.; Choi, J.-I. Analysis of Novel Antioxidant Sesquiterpenes (C35 Terpenes) Produced in Recombinant *Corynebacterium glutamicum*. *Appl. Biochem. Biotechnol.* **2018**, *186*, 525–534. [CrossRef]
29. Lim, H.; Park, J.; Woo, H.M. Overexpression of the Key Enzymes in the Methylerythritol 4-Phosphate Pathway in *Corynebacterium glutamicum* for Improving Farnesyl Diphosphate-Derived Terpene Production. *J. Agric. Food Chem.* **2020**, *68*, 10780–10786. [CrossRef]
30. Henke, N.A.; Austermeier, S.; Grothaus, I.L.; Götter, S.; Persicke, M.; Peters-Wendisch, P.; Wendisch, V.F. *Corynebacterium glutamicum* CrtR and Its Orthologs in *Actinobacteria*: Conserved Function and Application as Genetically Encoded Biosensor for Detection of Geranylgeranyl Pyrophosphate. *Int. J. Mol. Sci.* **2020**, *21*, 5482. [CrossRef]
31. Göttl, V.L.; Pucker, B.; Wendisch, V.F.; Henke, N.A. Screening of Structurally Distinct Lycopene  $\beta$ -Cyclases for Production of the Cyclic C40 Carotenoids  $\beta$ -Carotene and Astaxanthin by *Corynebacterium glutamicum*. *J. Agric. Food Chem.* **2023**, *71*, 7765–7776. [CrossRef] [PubMed]
32. Göttl, V.L.; Schmitt, I.; Braun, K.; Peters-Wendisch, P.; Wendisch, V.F.; Henke, N.A. CRISPRi-Library-Guided Target Identification for Engineering Carotenoid Production by *Corynebacterium glutamicum*. *Microorganisms* **2021**, *9*, 670. [CrossRef] [PubMed]
33. Henke, N.A.; Wiebe, D.; Pérez-García, F.; Peters-Wendisch, P.; Wendisch, V.F. Coproduction of Cell-Bound and Secreted Value-Added Compounds: Simultaneous Production of Carotenoids and Amino Acids by *Corynebacterium glutamicum*. *Bioresour. Technol.* **2018**, *247*, 744–752. [CrossRef] [PubMed]



34. Schmitt, I.; Meyer, F.; Krahn, I.; Henke, N.A.; Peters-Wendisch, P.; Wendisch, V.F. From Aquaculture to Aquaculture: Production of the Fish Feed Additive Astaxanthin by *Corynebacterium glutamicum* Using Aquaculture Sidestream. *Molecules* **2023**, *28*, 1996. [CrossRef] [PubMed]
35. Liu, J.; Xu, J.-Z.; Rao, Z.-M.; Zhang, W.-G. Industrial Production of L-Lysine in *Corynebacterium glutamicum*: Progress and Prospects. *Microbiol. Res.* **2022**, *262*, 127101. [CrossRef]
36. Hirasawa, T.; Wachi, M. Glutamate Fermentation-2: Mechanism of L-Glutamate Overproduction in *Corynebacterium glutamicum*. In *Amino Acid Fermentation*; Yokota, A., Ikeda, M., Eds.; Advances in Biochemical Engineering/Biotechnology; Springer: Tokyo, Japan, 2017; pp. 57–72, ISBN 978-4-431-56520-8.
37. Kircher, M.; Pfefferle, W. The Fermentative Production of L-Lysine as an Animal Feed Additive. *Chemosphere* **2001**, *43*, 27–31. [CrossRef] [PubMed]
38. Kiefer, D.; Merkel, M.; Lilge, L.; Hausmann, R.; Henkel, M. High Cell Density Cultivation of *Corynebacterium glutamicum* on Bio-Based Lignocellulosic Acetate Using pH-Coupled Online Feeding Control. *Bioresour. Technol.* **2021**, *340*, 125666. [CrossRef]
39. Knoll, A.; Bartsch, S.; Husemann, B.; Engel, P.; Schroer, K.; Ribeiro, B.; Stöckmann, C.; Seletzky, J.; Büchs, J. High Cell Density Cultivation of Recombinant Yeasts and Bacteria under Non-Pressurized and Pressurized Conditions in Stirred Tank Bioreactors. *J. Biotechnol.* **2007**, *132*, 167–179. [CrossRef]
40. Kiefer, D.; Tadele, L.R.; Lilge, L.; Henkel, M.; Hausmann, R. High-Level Recombinant Protein Production with *Corynebacterium glutamicum* Using Acetate as Carbon Source. *Microb. Biotechnol.* **2022**, *15*, 2744–2757. [CrossRef]
41. Schewe, H.; Kreuzer, A.; Schmidt, I.; Schubert, C.; Schrader, J. High Concentrations of Biotechnologically Produced Astaxanthin by Lowering pH in a *Phaffia rhodozyma* Bioprocess. *Biotechnol. Bioproc. E* **2017**, *22*, 319–326. [CrossRef]
42. Mandenius, C.-F.; Brundin, A. Bioprocess Optimization Using Design-of-Experiments Methodology. *Biotechnol. Prog.* **2008**, *24*, 1191–1203. [CrossRef]
43. Park, P.K.; Cho, D.H.; Kim, E.Y.; Chu, K.H. Optimization of Carotenoid Production by *Rhodotorula glutinis* Using Statistical Experimental Design. *World J. Microbiol. Biotechnol.* **2005**, *21*, 429–434. [CrossRef]
44. Prell, C.; Burgardt, A.; Meyer, F.; Wendisch, V.F. Fermentative Production of L-2-Hydroxyglutarate by Engineered *Corynebacterium glutamicum* via Pathway Extension of L-Lysine Biosynthesis. *Front. Bioeng. Biotechnol.* **2021**, *8*, 630476. [CrossRef]
45. Pérez-Rodríguez, N.; Pinheiro de Souza Oliveira, R.; Torrado Agrasar, A.M.; Domínguez, J.M. Ferulic Acid Transformation into the Main Vanilla Aroma Compounds by *Amycolatopsis* sp. ATCC 39116. *Appl. Microbiol. Biotechnol.* **2016**, *100*, 1677–1689. [CrossRef] [PubMed]
46. Follmann, M.; Ochrombel, I.; Krämer, R.; Trötschel, C.; Poetsch, A.; Rückert, C.; Hüser, A.; Persicke, M.; Seiferling, D.; Kalinowski, J.; et al. Functional Genomics of pH Homeostasis in *Corynebacterium glutamicum* Revealed Novel Links between pH Response, Oxidative Stress, Iron Homeostasis and Methionine Synthesis. *BMC Genom.* **2009**, *10*, 621. [CrossRef]
47. Bertani, G. STUDIES ON LYSOGENESIS I: The Mode of Phage Liberation by Lysogenic *Escherichia coli*. *J. Bacteriol.* **1951**, *62*, 293–300. [CrossRef] [PubMed]
48. Eggeling, L.; Reyes, O. Experiments. In *Handbook of Corynebacterium glutamicum*; CRC Press: Boca Raton, FL, USA, 2005; pp. 3535–3566.
49. Henke, N.A.; Frohwitter, J.; Peters-Wendisch, P.; Wendisch, V.F. Carotenoid Production by Recombinant *Corynebacterium glutamicum*: Strain Construction, Cultivation, Extraction, and Quantification of Carotenoids and Terpenes. In *Microbial Carotenoids: Methods and Protocols*; Barreiro, C., Barredo, J.-L., Eds.; Methods in Molecular Biology; Springer: New York, NY, USA, 2018; pp. 127–141, ISBN 978-1-4939-8742-9.
50. Lenth, R.V. Response-Surface Methods in R, Using Rsm. *J. Stat. Softw.* **2010**, *32*, 1–17. [CrossRef]
51. Lenth, R. Response-Surface Analysis. 2021. Available online: <https://cran.r-project.org/package=rsm> (accessed on 10 November 2023).
52. Jakob, K.; Satorhelyi, P.; Lange, C.; Wendisch, V.F.; Silakowski, B.; Scherer, S.; Neuhaus, K. Gene Expression Analysis of *Corynebacterium glutamicum* Subjected to Long-Term Lactic Acid Adaptation. *J. Bacteriol.* **2007**, *189*, 5582–5590. [CrossRef]
53. Täuber, S.; Blöbaum, L.; Wendisch, V.F.; Grünberger, A. Growth Response and Recovery of *Corynebacterium glutamicum* Colonies on Single-Cell Level Upon Defined pH Stress Pulses. *Front. Microbiol.* **2021**, *12*, 711893.
54. Lu, Q.; Liu, J.-Z. Enhanced Astaxanthin Production in *Escherichia coli* via Morphology and Oxidative Stress Engineering. *J. Agric. Food Chem.* **2019**, *67*, 11703–11709. [CrossRef]
55. Cho, J.-C.; Giovannoni, S.J. *Fulvimarina pelagi* gen. nov., sp. nov., a Marine Bacterium That Forms a Deep Evolutionary Lineage of Descent in the Order “Rhizobiales”. *Int. J. Syst. Evol. Microbiol.* **2003**, *53*, 1853–1859. [CrossRef]
56. Lajoie, C.A.; Kitner, J.B.; Potochnik, S.J.; Townsend, J.M.; Beatty, C.C.; Kelly, C.J. Cloning, Expression and Characterization of Xylose Isomerase from the Marine Bacterium *Fulvimarina pelagi* in *Escherichia coli*. *Biotechnol. Prog.* **2016**, *32*, 1230–1237. [CrossRef]
57. Garcia-Soto, C.; Cheng, L.; Caesar, L.; Schmidtko, S.; Jewett, E.B.; Cheripka, A.; Rigor, I.; Caballero, A.; Chiba, S.; Báez, J.C.; et al. An Overview of Ocean Climate Change Indicators: Sea Surface Temperature, Ocean Heat Content, Ocean pH, Dissolved Oxygen Concentration, Arctic Sea Ice Extent, Thickness and Volume, Sea Level and Strength of the AMOC (Atlantic Meridional Overturning Circulation). *Front. Mar. Sci.* **2021**, *8*, 642372.
58. Fraser, P.D.; Miura, Y.; Misawa, N. In Vitro Characterization of Astaxanthin Biosynthetic Enzymes \*. *J. Biol. Chem.* **1997**, *272*, 6128–6135. [CrossRef]



59. Bouvier, F.; Keller, Y.; d'Harlingue, A.; Camara, B. Xanthophyll Biosynthesis: Molecular and Functional Characterization of Carotenoid Hydroxylases from Pepper Fruits (*Capsicum annuum* L.). *Biochim. Biophys. Acta* **1998**, *1391*, 320–328. [[CrossRef](#)]
60. Hirasawa, K.; Yoneda, H.; Yata, T.; Azuma, M. Method for Producing Astaxanthin by Fermentation 2013. US patent US20130012594A1, 22 December 2014.
61. Zhang, M.; Gong, Z.; Tang, J.; Lu, F.; Li, Q.; Zhang, X. Improving Astaxanthin Production in *Escherichia coli* by Co-Utilizing CrtZ Enzymes with Different Substrate Preference. *Microb. Cell Factories* **2022**, *21*, 71. [[CrossRef](#)]
62. Gong, Z.; Wang, H.; Tang, J.; Bi, C.; Li, Q.; Zhang, X. Coordinated Expression of Astaxanthin Biosynthesis Genes for Improved Astaxanthin Production in *Escherichia coli*. *J. Agric. Food Chem.* **2020**, *68*, 14917–14927. [[CrossRef](#)]
63. Kwak, H.S.; Kim, J.Y.H.; Sim, S.J. A Microreactor System for Cultivation of *Haematococcus pluvialis* and Astaxanthin Production. *J. Nanosci. Nanotechnol.* **2015**, *15*, 1618–1623. [[CrossRef](#)] [[PubMed](#)]
64. Ahmad, M.N.; Holland, C.R.; McKay, G. Mass Transfer Studies in Batch Fermentation: Mixing Characteristics. *J. Food Eng.* **1994**, *23*, 145–158. [[CrossRef](#)]
65. Nyiri, L.; Lengyel, Z.L. Studies on Ventilation of Culture Broths. I. Behavior of CO<sub>2</sub> in Model Systems. *Biotechnol. Bioeng.* **1968**, *10*, 133–150. [[CrossRef](#)]
66. Royce, P.N.C.; Thornhill, N.F. Estimation of Dissolved Carbon Dioxide Concentrations in Aerobic Fermentations. *AIChE J.* **1991**, *37*, 1680–1686. [[CrossRef](#)]
67. Bäumchen, C.; Knoll, A.; Husemann, B.; Seletzky, J.; Maier, B.; Dietrich, C.; Amoabediny, G.; Büchs, J. Effect of Elevated Dissolved Carbon Dioxide Concentrations on Growth of *Corynebacterium glutamicum* on D-Glucose and L-Lactate. *J. Biotechnol.* **2007**, *128*, 868–874. [[CrossRef](#)]
68. Buchholz, J.; Graf, M.; Freund, A.; Busche, T.; Kalinowski, J.; Blombach, B.; Takors, R. CO<sub>2</sub>/HCO<sub>3</sub><sup>−</sup> Perturbations of Simulated Large Scale Gradients in a Scale-down Device Cause Fast Transcriptional Responses in *Corynebacterium glutamicum*. *Appl. Microbiol. Biotechnol.* **2014**, *98*, 8563–8572. [[CrossRef](#)]
69. Blombach, B.; Buchholz, J.; Busche, T.; Kalinowski, J.; Takors, R. Impact of Different CO<sub>2</sub>/HCO<sub>3</sub><sup>−</sup> Levels on Metabolism and Regulation in *Corynebacterium glutamicum*. *J. Biotechnol.* **2013**, *168*, 331–340. [[CrossRef](#)]
70. Müller, F.; Rapp, J.; Hacker, A.-L.; Feith, A.; Takors, R.; Blombach, B. CO<sub>2</sub>/HCO<sub>3</sub><sup>−</sup> Accelerates Iron Reduction through Phenolic Compounds. *mBio* **2020**, *11*, e00085-20. [[CrossRef](#)]
71. Zepeck, F.; Gräwert, T.; Kaiser, J.; Schramek, N.; Eisenreich, W.; Bacher, A.; Rohdich, F. Biosynthesis of Isoprenoids. Purification and Properties of IspG Protein from *Escherichia coli*. *J. Org. Chem.* **2005**, *70*, 9168–9174. [[CrossRef](#)] [[PubMed](#)]
72. Rückert, C.; Koch, D.J.; Rey, D.A.; Albersmeier, A.; Mormann, S.; Pühler, A.; Kalinowski, J. Functional Genomics and Expression Analysis of the *Corynebacterium glutamicum* *fpr2-cysIXHDNYZ* Gene Cluster Involved in Assimilatory Sulphate Reduction. *BMC Genom.* **2005**, *6*, 121. [[CrossRef](#)]
73. Isenschmid, A.; Marison, I.W.; von Stockar, U. The Influence of Pressure and Temperature of Compressed CO<sub>2</sub> on the Survival of Yeast Cells. *J. Biotechnol.* **1995**, *39*, 229–237. [[CrossRef](#)]
74. Seel, W.; Baust, D.; Sons, D.; Albers, M.; Eitzbach, L.; Fuss, J.; Lipski, A. Carotenoids Are Used as Regulators for Membrane Fluidity by *Staphylococcus xylosum*. *Sci. Rep.* **2020**, *10*, 330. [[CrossRef](#)]
75. Wu, T.; Ye, L.; Zhao, D.; Li, S.; Li, Q.; Zhang, B.; Bi, C.; Zhang, X. Membrane Engineering—A Novel Strategy to Enhance the Production and Accumulation of β-Carotene in *Escherichia coli*. *Metab. Eng.* **2017**, *43*, 85–91. [[CrossRef](#)]
76. Follonier, S.; Escapa, I.F.; Fonseca, P.M.; Henes, B.; Panke, S.; Zinn, M.; Prieto, M.A. New Insights on the Reorganization of Gene Transcription in *Pseudomonas putida* KT2440 at Elevated Pressure. *Microb. Cell Factories* **2013**, *12*, 30. [[CrossRef](#)] [[PubMed](#)]
77. Dixon, N.M.; Kell, D.B. The Inhibition by CO<sub>2</sub> of the Growth and Metabolism of Micro-Organisms. *J. Appl. Bacteriol.* **1989**, *67*, 109–136. [[CrossRef](#)] [[PubMed](#)]
78. Basiony, M.; Ouyang, L.; Wang, D.; Yu, J.; Zhou, L.; Zhu, M.; Wang, X.; Feng, J.; Dai, J.; Shen, Y.; et al. Optimization of Microbial Cell Factories for Astaxanthin Production: Biosynthesis and Regulations, Engineering Strategies and Fermentation Optimization Strategies. *Synth. Syst. Biotechnol.* **2022**, *7*, 689–704. [[CrossRef](#)]
79. Ramírez, J.; Gutierrez, H.; Gschaedler, A. Optimization of Astaxanthin Production by *Phaffia rhodozyma* through Factorial Design and Response Surface Methodology. *J. Biotechnol.* **2001**, *88*, 259–268. [[CrossRef](#)] [[PubMed](#)]
80. Carsanba, E.; Pintado, M.; Oliveira, C. Fermentation Strategies for Production of Pharmaceutical Terpenoids in Engineered Yeast. *Pharmaceuticals* **2021**, *14*, 295. [[CrossRef](#)] [[PubMed](#)]
81. Morschett, H.; Jansen, R.; Neuendorf, C.; Moch, M.; Wiechert, W.; Oldiges, M. Parallelized Microscale Fed-Batch Cultivation in Online-Monitored Microtiter Plates: Implications of Media Composition and Feed Strategies for Process Design and Performance. *J. Ind. Microbiol. Biotechnol.* **2020**, *47*, 35–47. [[CrossRef](#)] [[PubMed](#)]
82. Jia, D.; Xu, S.; Sun, J.; Zhang, C.; Li, D.; Lu, W. *Yarrowia lipolytica* Construction for Heterologous Synthesis of α-Santalene and Fermentation Optimization. *Appl. Microbiol. Biotechnol.* **2019**, *103*, 3511–3520. [[CrossRef](#)] [[PubMed](#)]
83. Chang, H.N.; Kim, N.-J.; Kang, J.; Jeong, C.M.; Choi, J.; Fei, Q.; Kim, B.J.; Kwon, S.; Lee, S.Y.; Kim, J. Multi-Stage High Cell Continuous Fermentation for High Productivity and Titer. *Bioprocess. Biosyst. Eng.* **2011**, *34*, 419–431. [[CrossRef](#)]
84. Gupta, V.; Odaneth, A.A.; Lali Arvind, M. High Cell Density Continuous Fermentation for L-Lactic Acid Production from Cane Molasses. *Prep. Biochem. Biotechnol.* **2023**, *53*, 1043–1057. [[CrossRef](#)]
85. Mei, Y.; Yang, Z.; Kang, Z.; Yu, F.; Long, X. Enhanced Surfactin Fermentation via Advanced Repeated Fed-Batch Fermentation with Increased Cell Density Stimulated by EDTA–Fe (II). *Food Bioprod. Process.* **2021**, *127*, 288–294. [[CrossRef](#)]

- 
86. Riesenberg, D.; Guthke, R. High-Cell-Density Cultivation of Microorganisms. *Appl. Microbiol. Biotechnol.* **1999**, *51*, 422–430. [[CrossRef](#)]
  87. Neubauer, P.; Junne, S. Scale-Up and Scale-Down Methodologies for Bioreactors. In *Bioreactors*; John Wiley & Sons, Ltd.: Hoboken, NJ, USA, 2016; pp. 323–354, ISBN 978-3-527-68336-9.

**Disclaimer/Publisher’s Note:** The statements, opinions and data contained in all publications are solely those of the individual author(s) and contributor(s) and not of MDPI and/or the editor(s). MDPI and/or the editor(s) disclaim responsibility for any injury to people or property resulting from any ideas, methods, instructions or products referred to in the content.